Research Square

Preprints are preliminary reports that have not undergone peer review.
They should not be considered conclusive, used to inform clinical practice,
or referenced by the media as validated information.

Surface Roughness Evolution and Tool-Wear Mechanisms in Prolonged Milling of Ti6Al4V ELI under Sunflower-Oil and MoS_2-Enhanced MQL Environments

Deniz ÇOBAN ÖZKAN

deniz.coban@cbu.edu.tr

Manisa Celal Bayar University: Manisa Celal Bayar Universitesi

Fikret Sönmez

Manisa Celal Bayar University: Manisa Celal Bayar Universitesi

Research Article

Keywords: Ti6Al4V ELI, minimum quantity lubrication, sunflower oil, MoS_2 nanoparticles, tool wear, surface roughness

Posted Date: August 19th, 2026

DOI: https://doi.org/10.21203/rs.3.rs-10577069/v1

License: This work is licensed under a Creative Commons Attribution 4.0 International License.
Read Full License

Surface Roughness Evolution and Tool-Wear Mechanisms in Prolonged Milling of Ti6Al4V ELI under Sunflower-Oil and MoS_2-Enhanced MQL Environments

Deniz ÇOBAN ÖZKAN[1], Fikret SÖNMEZ[1,*]

[1]Department of Mechanical Engineering, Hasan Ferdi Turgutlu Faculty of Technology, Manisa Celal Bayar University, Manisa, Turkey

*** Corresponding author at:** Department of Mechanical Engineering, Hasan Ferdi Turgutlu Faculty of Technology, Manisa Celal Bayar University, Manisa, 45400, Turkey **E-mail address:** sonmezfikret@gmail.com (fikret.sonmez@cbu.edu.tr)

Deniz ÇOBAN ÖZKAN 0000-0002-8044-5952

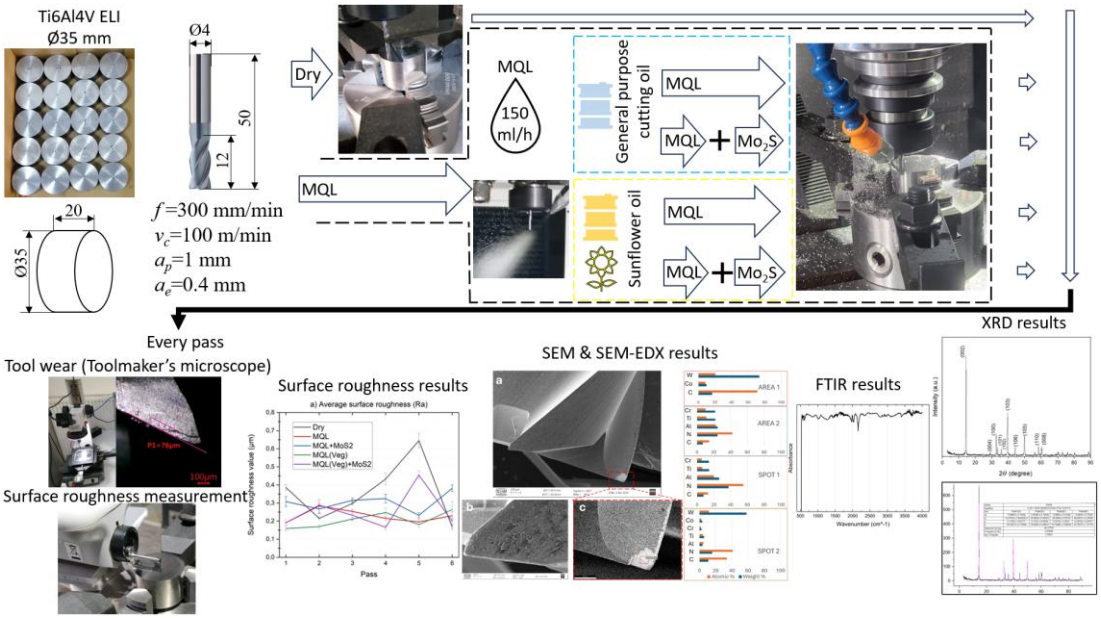
Fikret SÖNMEZ 0000-0003-1718-892X

ABSTRACT

Ti6Al4V ELI (Grade 23) is widely used in aerospace and biomedical applications due to its high strength-to-weight ratio and biocompatibility. However, low thermal conductivity, high chemical affinity, and built-up edge (BUE) formation degrade its machinability, necessitating effective lubrication. This study evaluates the effects of five environments — dry cutting, conventional MQL, sunflower oil-based MQL, and their MoS_2 nanoparticle-reinforced variants — on surface roughness and tool wear during face milling under a sustained 84-minute protocol. Surface roughness (Ra, Rz) and flank wear were monitored progressively using a profilometer and toolmaker's microscope, while tool wear mechanisms and MoS_2 nanoparticles were characterized via SEM-EDX, FTIR, XRD, and XPS. To the best of the authors' knowledge, this is the first study to combine sunflower-oil-based MQL with MoS_2 nanoparticles for Ti6Al4V ELI (Grade 23) under a prolonged (84-min) milling protocol and to statistically resolve the lubrication–pass-number interaction governing surface roughness evolution. Two-way ANOVA confirmed significant interaction effects of lubrication and pass number on Ra. Sunflower oil-based MQL yielded the lowest Ra (0.159 µm), a 75% reduction from dry cutting (0.645 µm), whereas MoS_2 addition showed no statistically significant surface finish improvement. Conversely, dry cutting caused severe edge fracture and a maximum flank wear of 252 µm. SEM-EDX revealed that MoS_2 nanoparticles suppressed BUE and coating delamination, confirming their primary benefit lies in tool preservation rather than surface finish enhancement, supporting vegetable oil-based MQL as a sustainable machining alternative.

Keywords: Ti6Al4V ELI; minimum quantity lubrication; sunflower oil; MoS_2 nanoparticles; tool wear; surface roughness

Graphical abstract



1. Introduction

Machining is a superior manufacturing technique due to its excellent dimensional and geometric accuracy as well as its ability to achieve exceptionally low surface roughness. However, the machining of titanium alloys, particularly Ti6Al4V ELI, inherently involves extreme tribological conditions at the tool-chip and tool-workpiece interfaces. These conditions are characterized by severe contact pressures, highly localized temperatures, and the continuous exposure of highly reactive, unoxidized metal surfaces, leading to severe adhesive and diffusion wear. Under such severe thermomechanical interactions, intense friction and rapid tool degradation are unavoidable [1-4].

During machining, significant heat generation and frictional forces develop at the cutting zone. Under severe thermomechanical loading conditions, material transferred from the workpiece may adhere to the tool surface [5]. Cooling fluids are utilized to mitigate the detrimental effects of such contact and friction on the cutting tool and workpiece, even though these situations are unavoidable according to machining principles. Traditional flood cooling systems, while effective, raise environmental and occupational health concerns. Minimum Quantity Lubrication (MQL) is an alternative, environmentally friendly, and effective cooling method that delivers a small amount of coolant (typically in the range of 50-250 ml/hour) directly to the cutting zone in an atomized form. To further enhance the performance of the MQL method, several strategies are employed, including the addition of different particle sizes (particle reinforcement) and various types of cutting fluids [6-9].

Titanium alloys are distinguished by their exceptional strength and wear resistance, as well as their extremely low density (4.43 g/cm³), which makes them an effective alternative to many industrial materials, especially steels. Ti6Al4V ELI (Extra Low Interstitials) (Grade 23), a variant of the widely used Ti6Al4V (Grade 5), has fewer interstitial atoms (mainly oxygen and carbon). This titanium alloy's superior biocompatibility and resistance to corrosion make it a primary material utilized in bioengineering and aerospace [10, 11]. Given its widespread industrial significance, numerous studies have focused on optimizing the machining parameters of titanium alloys under various lubrication conditions.

Sarma et al. [12] conducted 27 different experiments using machine-learning approaches (support vector regression (SVR) and Jaya optimization) to investigate the effect of feed on surface roughness during the machining of Ti6Al4V alloy under MQL conditions. The optimum machining parameters were determined as a cutting speed of 120 m/min, a feed of 0.05 mm/rev, and a 0.2 mm depth of cut. A significant reduction in surface roughness was obtained with optimum conditions compared to other conditions, reducing the Ra value to 0.4812 μm. Feed was identified as the most significant parameter, whereas cutting speed had a limited effect, and depth of cut showed no significant impact. The error (MAPE) was calculated as 4.68%.

Ni et al. [13] investigated the surface roughness of Ti6Al4V alloys machined under dry and MQL conditions. The researchers used a Toshiba ULG-100 ultra-precision machine equipped with a carbide insert. The MQL application resulted in a considerable enhancement in surface roughness of 62.3–82.2% compared to dry cutting.

Swain et al. [14] reported that in a study on CNC turning of Ti–6Al–4V alloy, when dry and MQL conditions were compared, tool wear decreased by approximately 67%, tool life increased by 280%, and total cutting costs decreased by 12.38% with the application of MQL.

Recently, studies on the addition of nanoparticles to cooling fluids in MQL systems—referred to in the literature as NFMQL (Nano Fluid Minimum Quantity Lubrication)—have gained attention. The machining of

various metals using NFMQL with nanoparticles such as aluminum oxide (Al_2O_3), graphene, copper oxide (CuO), and molybdenum disulfide (MoS_2) has been investigated.

For instance, Yücel et al. [15] compared dry cutting, pure MQL, and MoS_2-enriched NFMQL methods in the turning of AA2024-T3 aluminum alloy. A Taguchi L27 orthogonal array was used in the experimental design, and surface roughness, maximum temperature, surface topography, and BUE/BUL formation on the tool were examined using SEM-EDX. The results showed an 8.41% improvement in surface roughness with MQL compared to dry machining and a 15.56% improvement with MoS_2-added NFMQL. In the experiments, cutting temperatures were reduced by 10.21% with MQL and by 22.44% with NFMQL. Particularly with the NFMQL application, a significant suppression of BUE/BUL formations was observed, resulting in less damaged tool edges and smoother surfaces. Sahoo and Datta [16] reported that the nanofluid-MQL application using graphene nanoplatelet-modified Jatropha oil provided more effective cooling and lubrication. In their experiments, superior results were observed in the machining of Ti–6Al–4V alloy compared to dry and conventional MQL, significantly reducing tool wear at cutting speeds up to 82 m/min and improving surface roughness at speeds up to 106 m/min.

Şen et al. [17] studied the milling of Inconel 690 using a nanofluid-MQL application with palm oil containing Al_2O_3. They demonstrated that a 0.9% Al_2O_3 ratio reduced tool wear by 19.35% compared to flood cooling and by 10.71% compared to pure MQL. The researchers observed that this method also limited wear by forming a protective tribofilm on the surface. Jyothish et al. [18] investigated the machining of Inconel-718 with MQL by adding $ZnTiO_3$, BN, and CuO nanoparticles to a sunflower oleic acid-based cutting fluid. The researchers developed nanofluids that showed improvements of up to 70% in thermal conductivity with BN addition and up to 30% in viscosity with $ZnTiO_3$ addition. Junankar et al. [19] compared CuO and ZnO-containing nanofluid-MQL fluids in the turning of bearing steel. The researchers reported that the CuO nanofluid-MQL reduced surface roughness by 38% and machining temperature by 12%. Overall, these studies suggest that the effectiveness of nanoparticle additives is highly system-dependent, being influenced by the base-oil chemistry, the particle type and concentration, and the specific workpiece–tool combination. This highlights the need for material-specific investigations rather than drawing generalized conclusions. Azami et al. [20] claimed that nano-MQL applied with MoS_2 and CuO-containing vegetable oils significantly improved performance during the grinding of AISI D2 steel. The normal force was reduced by approximately 31% with the soybean oil and 4% CuO combination, while surface roughness decreased by 70% with the rapeseed oil and 2% CuO combination.

Gnanavel et al. [21] compared conventional sustainable machining methods with nanofluid-MQL containing waste cooking oil and MoS_2 nanoparticles used in the turning of SAE1144 steel. Using a Taguchi L16 experimental design, they reported that the nanofluid-MQL application reduced average tool wear by 38% and that the best results were obtained under low cutting speed (40 m/min) and low feed (0.05 mm/rev) conditions.

Xu et al. [5] investigated the formation of the adhesive layer and its dual role in the tribological performance and surface integrity of Ti-6Al-4V alloy during machining under dry and MQL conditions. By analyzing the physical and mechanistic behaviors of the adhesive layer, the researchers reported that this layer acts as a protective barrier on the cutting tool, reducing contact pressure and friction due to its low elastic modulus. However, the researchers also highlighted that its instability significantly deteriorates surface integrity by increasing surface roughness (Rz) and inducing a substantial work-hardened layer beneath the machined surface.

In the machining of Ti6Al4V alloys, it has been clearly demonstrated in the literature that MQL applications offer significant advantages over dry machining in terms of reducing tool wear, extending tool life, improving surface integrity, and lowering production costs.

Although the beneficial effects of MQL and nanoparticle-assisted MQL on the machining performance of titanium alloys have been widely reported, several important research gaps remain. First, the majority of previous studies have focused on the conventional Ti6Al4V Grade 5 alloy, whereas investigations concerning Ti6Al4V ELI (Grade 23) remain comparatively limited despite its increasing utilization in biomedical and aerospace applications. Due to its lower interstitial content and different mechanical characteristics, the tribological behavior and machinability of Grade 23 cannot be assumed to be identical to those of Grade 5.

Second, although various vegetable oils and nanoparticle additives have been investigated as environmentally friendly lubricants, the combined application of sunflower oil and MoS_2 nanoparticles under MQL conditions has received very limited attention in the machining of Ti6Al4V ELI. Most available studies have focused on alternative vegetable oils, different nanoparticle systems, or materials other than titanium alloys.

Third, previous investigations have generally evaluated machining performance under relatively short machining durations. Consequently, limited information is available regarding the long-term evolution of tool wear and surface integrity under sustained machining conditions. Progressive wear mechanisms, coating degradation, and built-up edge formation may exhibit substantially different behavior during extended machining periods compared with short-duration experiments.

Fourth, although surface roughness and tool wear have frequently been reported independently, the interaction between lubrication strategy and machining progression has rarely been examined through a statistically rigorous framework. In particular, the influence of pass number and its interaction with lubrication conditions on surface roughness evolution remains insufficiently understood.

To address these gaps, the present study investigates the face milling of Ti6Al4V ELI (Grade 23) under five different cooling/lubrication environments, including dry machining, conventional MQL, sunflower-oil-based MQL, and MoS_2-enhanced variants. Unlike many previous studies, the experiments were conducted under an extended machining duration of approximately 84 minutes to enable the assessment of progressive wear behavior. Furthermore, the effects of lubrication condition and pass number on surface roughness were evaluated using two-way ANOVA and Tukey HSD analyses, while the underlying wear mechanisms were investigated through SEM-EDX examinations. In addition, the MoS_2 nanoparticles were comprehensively characterized using SEM, FTIR, XRD, and XPS analyses. The findings contribute to a better understanding of the tribological performance of sustainable lubrication strategies for machining Ti6Al4V ELI and clarify the role of MoS_2 nanoparticles in both surface quality and tool preservation. The main contributions of this work are threefold. First, it provides the first systematic comparison of five cooling/lubrication environments for Ti6Al4V ELI under an extended 84-min milling protocol. Second, two-way ANOVA and Tukey HSD analyses demonstrate that the effectiveness of each lubrication strategy strongly depends on the machining pass (interaction partial $\eta^2 = 0.822$). Finally, SEM-EDX observations indicate that MoS_2 nanoparticles mainly contribute to tool preservation by suppressing BUE formation and coating delamination, rather than by further improving surface finish.

2. Experimental Methods

2.1. Workpiece Material and Cutting Tool

In this study, Ti6Al4V ELI (Grade 23) alloy was used. Ti6Al4V ELI (Grade 23) contains fewer interstitial elements, especially carbon and oxygen, than Ti6Al4V (Grade 5). As a result, it exhibits increased fracture toughness and ductility. The chemical and mechanical properties are provided in Table 1.

Table 1 The chemical and mechanical properties of Ti6Al4V ELI (Grade 23)

Element	Al	C	Fe	H	N	O	V	Ti
% weight	5.885	0.022	0.1	0.003	0.008	0.101	3.925	Balance

Mechanical properties	Tensile strength (MPa)	Yield strength (MPa)	Elongation %
Value	915	862	17.8

The Ti6Al4V ELI material was received as a Ø35 mm, cold-rolled bar (TiFast S.r.l., Italy) and cut to a length of 22 mm using a CNC turning center (Fig. 1a, Fig. 1b). After the turning operations, the workpieces were clamped by a three-jaw chuck on the CNC vertical machining center (Fig. 1c). A Ø4 mm solid carbide end mill (C76 0400, HPMT, Malaysia) was employed in the research (Fig. 1d). The tool has 4 flutes, an overall length of 50 mm, and a cutting length of 12 mm, coated with AlCrN (H6110). The tool has an unequal, variable helix (35°-40°) to minimize chatter.

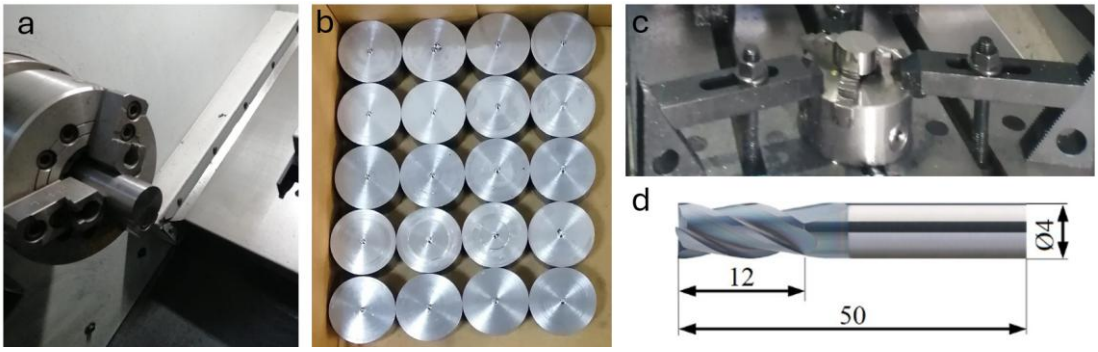


Fig. 1 Preparation of workpieces a) Cutting process on CNC lathe b) Cut workpieces c) The setup on a CNC Milling machine d) The cutting tool

2.2 Experimental Procedure and Machining Parameters

Before performing the experiments, several preliminary studies were conducted to determine the optimal cutting parameters based on the literature. As a result, a cutting speed (Vc) of 100 m/min, a depth of cut (ap) of 1 mm, a radial depth of cut (ae) of 0.4 mm, and a table feed of 300 mm/min (corresponding to a feed per tooth of fz ≈ 0.0094 mm/tooth for the four-flute tool at 7958 rpm) were established. The tool overhang length was set to 25 mm for the experiments. The entire circular top face (Ø35 mm) of the workpieces was machined using the down-milling (climb milling) strategy. To remove a total material thickness of 6 mm from the workpiece, the face milling operation was repeated in six successive axial layers (6 passes with 1 mm ap). Due to the small radial engagement

(ae= 0.4 mm), the total cumulative machining time to complete one workpiece reached approximately 84 minutes, providing a robust condition for evaluating steady-state tool wear.

In addition to dry machining conditions, the experiments were performed in four distinct cooling/lubrication conditions: MQL with cutting fluid (Werte Fastcut Ultra), MQL with cutting fluid and nanoparticle additives, MQL with sunflower oil, and MQL with sunflower oil and nanoparticle additives. Table 2 lists the lubricating and cooling environments. To eliminate the influence of prior wear and ensure experimental consistency, a dedicated cutting tool was assigned to each lubrication condition, and all six machining passes were performed using the same tool under that specific condition.

Table 2 Cooling/lubrication environments

Cooling/Lubrication Environment	Flow Rate	Nanoparticle Addition
Dry	-	-
General-purpose cutting fluid (Werte Fastcut Ultra), MQL	150 ml/hour	-
General-purpose cutting fluid with nanoparticle-enhanced MQL	150 ml/hour	0.5 vol.% (MoS_2)
Sunflower oil-based MQL	150 ml/hour	-
Sunflower oil-based nanoparticle-enhanced MQL	150 ml/hour	0.5 vol.% (MoS_2)

The objective of the present study was not to optimize machining parameters but rather to evaluate the long-term tribological performance of different lubrication strategies under a representative machining condition. Ti6Al4V ELI is characterized by low thermal conductivity and high chemical affinity with cutting tool materials, which promote progressive tool degradation during machining. The selected cutting conditions were based on preliminary trials and correspond to the manufacturer's recommended operating range for Ti6Al4V machining. Therefore, a constant cutting parameter set was intentionally selected to isolate the influence of lubrication conditions and to monitor wear evolution over an extended machining period of approximately 84 minutes. This approach enabled a direct comparison of the cooling and lubrication capabilities of the investigated environments while minimizing the influence of additional process variables. Although broader machining parameter ranges should be considered in future studies, the selected methodology provides valuable insight into tool wear progression and surface integrity under sustained machining conditions that are relevant to industrial practice.

2.3 Preparation of Nanofluids and MQL Setup

In the study, cutting fluid and sunflower oil were used as received. Among the various nanoparticles utilized in MQL applications, molybdenum (IV) sulfide (MoS_2) is widely preferred due to its low friction coefficient at high temperatures [15, 20, 22]. MoS_2 with a nominal particle size of 2 µm and 98% purity (CAS number 1317-33-5 – Sigma-Aldrich) was used in the study. Prior to the experiments, the size of MoS_2 particles was examined using SEM. The analysis revealed that while the maximum particle size was approximately 2 µm, the majority of particles were distributed within the 200–400 nm range.

Previous studies have reported that nanoparticle concentrations around 0.5 vol.% frequently provide favorable tribological performance in nano-MQL applications and are commonly adopted in machining studies involving base cutting fluids (vegetable oil, cutting fluid, etc.) [16, 19, 22]. Therefore, a concentration of 0.5 vol.% was selected in the present work. The selected nanoparticle concentration was based on previously reported optimum or near-optimum values in nano-MQL studies. The objective of the present work was not to optimize nanoparticle concentration but rather to evaluate the tribological effectiveness of MoS_2-enhanced lubrication under prolonged machining conditions.

To prepare the nanofluids, MoS_2 was added to the base fluids. The required mass of MoS_2 was calculated to achieve a 0.5 vol.% concentration and subsequently dispersed into the base fluid. The mixture was then stirred for 60 min at 1500 rpm using a magnetic stirrer, and the nanoparticles were mechanically dispersed in the base fluid [23, 24]. Prior to each experiment, the nanofluid mixture was re-stirred to minimize possible particle sedimentation and to ensure a uniform distribution during the machining tests.

Each prepared fluid (Fig. 2a) was transferred to a Werte STN 15 MQL device (Werte, Turkey) for MQL applications (Fig. 2b), and the flow rate was adjusted to 150 ml/h at a carrier-air pressure of 6 bar for each fluid. The nozzle of the MQL device was positioned at a 45° angle and a distance of 30 mm relative to the cutting tool (Fig. 2c and Fig. 2d). Experiments were initiated once a stable lubrication supply rate was achieved. The technical properties of the base fluids and additives were obtained from the suppliers' technical/safety data sheets and are presented in Table 3.



Fig. 2 a) A prepared cutting fluid, b) MQL device, c) Stable MQL rate, d) Machining operation

Table 3 Properties of General-Purpose Cutting Oil, Sunflower Oil, and MoS_2 Nanoparticles

Properties	**General-Purpose Cutting Oil (Werte Fastcut Ultra)**	**Sunflower Oil**	**Nanoparticle (MoS_2)**
Flash Point (°C)	121	220	–
Boiling Point (°C)	215	350	–
Relative Density	0.91	0.92	5.06
Viscosity / Fluidity (cSt)	18	65.2	–
Vapor Pressure (mmHg @ 20 °C)	<0.01	<0.01	–
Vapor Density	>5	N/A	–
Particle Size	–	–	≤ 2 micron
Concentration	–	–	0.5% by volume

2.4 Measurements and Analysis

Tool wear and surface roughness were examined after each pass. Tool wear was inspected using a toolmaker's microscope (Mahr MarVision MM200, Göttingen, Germany) equipped with a 5 MP digital camera (Fig. 3a) on both the flank and the end faces of the tool (Fig. 3b and Fig. 3c). Five surface roughness measurements were taken at different locations and orientations on the workpiece after each pass to enable statistical analysis and quantify measurement variability. These five measurements per pass served as replicates in the statistical analysis. Full run-level replication was not performed, since each 84-min experiment consumes a dedicated tool and workpiece; this constraint is acknowledged in the Limitations and Future Work section. The average surface roughness (Ra) and maximum surface roughness (Rz) values were measured using a Bluetooth-enabled measuring device (Mahr MarSurf RD18, Göttingen, Germany) and a terminal unit (Mahr M300, Göttingen, Germany) as shown in Fig. 3d and Fig. 3e. Measurements were performed according to ISO 4287 using a cutoff length of 0.8 mm, an evaluation length of 4 mm, and total traversing length of 5.6 mm. After all passes, the worn tools were examined using SEM and EDX (Fig. 3f).

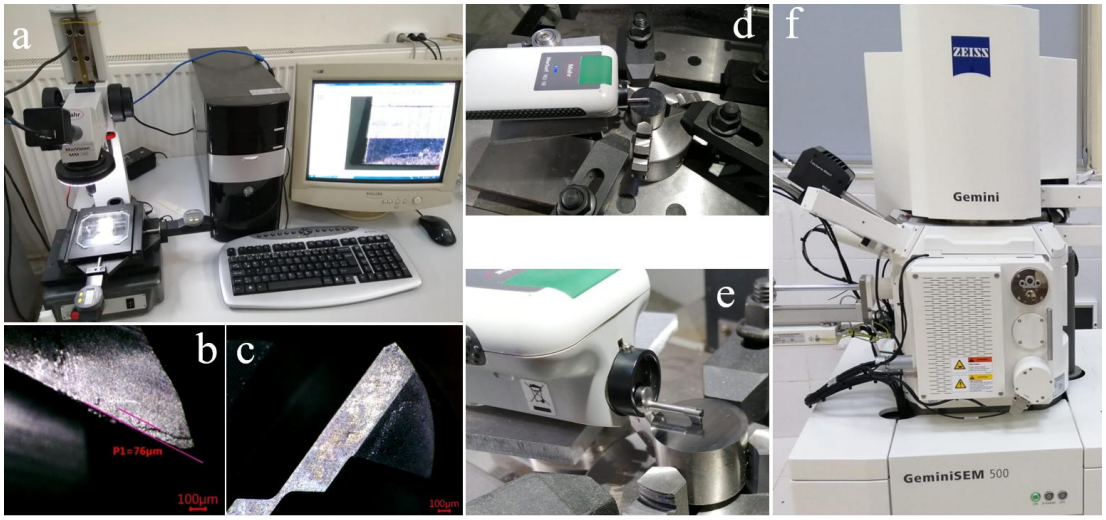


Fig. 3 a) Toolmaker's microscope, b) - c) tool measuring, d) surface roughness measurements, e) surface roughness measurements, f) SEM-EDX device

3. Results and Discussion

3.1. Characterization of the MoS_2 Nanoparticles

3.1.1 SEM analysis of the nanoparticle

In the particle size analysis (Fig. 4), it was observed that particle sizes varied. In the measurement results of some particles, dimensional measurements of 278.8 nm, 333.8 nm, and 379.8 nm were obtained. Examination of the SEM images reveals that the nanoparticles exhibit no agglomeration, confirming the absence of agglomeration in the dry state.

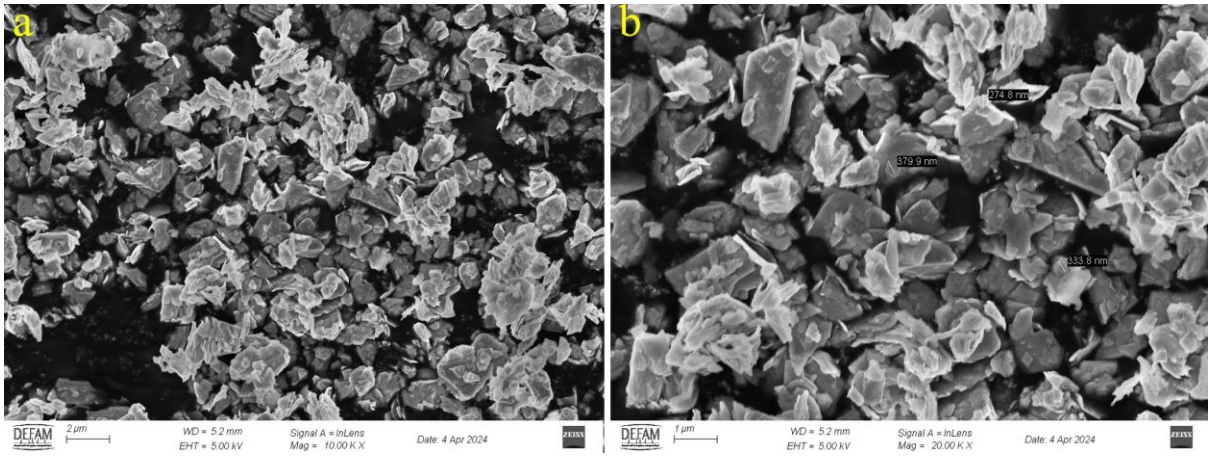


Fig. 4 The analysis of nano particles at a) 10k and b) 20k magnification

3.1.2. FTIR Analysis

The characterization of nanomaterials was also carried out with FTIR, XRD, and XPS analyses. The FTIR spectrum of molybdenum (IV) sulfide is presented in Fig. 5.

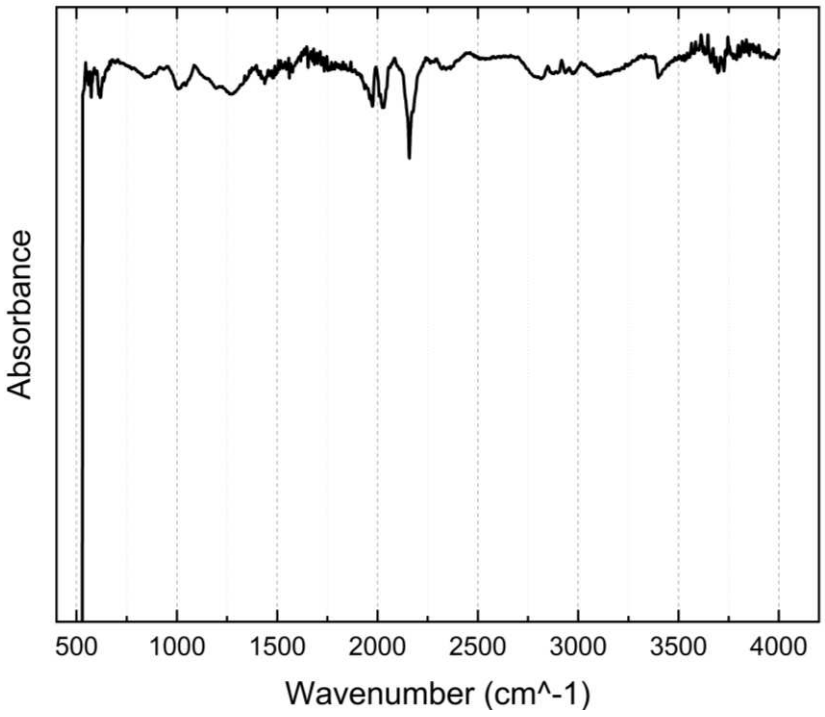


Fig. 5 MoS_2 FTIR Absorbance.

The absorption band observed at 3440 cm^{-1} is attributed to O–H stretching vibrations associated with adsorbed moisture on the particle surface [25]. The peak at 1720 cm^{-1} can be attributed to C=O stretching vibrations, which are probably caused by surface contamination or residual organic species that were introduced during synthesis or handling [25]. The absorption bands observed in the 700–1150 cm^{-1} region are commonly attributed to sulfate species [26]. Furthermore, the peaks observed at 620 and 1127 cm^{-1} have been reported to

correspond to Mo–S related vibrations in the literature [26, 27]. Collectively, the FTIR analysis confirms the presence of characteristic bonds associated with the MoS_2 nanomaterial.

3.1.3. XRD Analysis

The XRD pattern of molybdenum (IV) sulfide (MoS_2) is presented in Fig. 6. When the XRD data are examined, the positions of the diffraction peaks in the graph are observed at 14.14°, 28.50°, 32.92°, 33.71°, 35.89°, 39.58°, 44.12°, 49.51°, 55.53°, 58.53°, 60.69° and 62.15°. These peaks correspond to the hexagonal MoS_2 phase (JCPDS (ICCD) card no. 37-1492). The planes corresponding to each peak, respectively, are as follows: (002), (004), (100), (101), (102), (103), (006), (105), (106), (110), (008) and (112) [28]. It is possible to determine crystallite dimensions using XRD data via the Scherrer equation. The equation is defined as $D=K\lambda/(\beta\cos\theta)$, where D is the nanocrystallite size, λ is the wavelength (nm) of XRD radiation, and β is the full width at half maximum of the peaks in radians. The shape factor K ranges from 0.62 to 2.08 but is usually taken as 0.9 [29-31]. Based on the Scherrer equation, the average crystallite size was calculated as 40.74 nm, as detailed in Table 4.

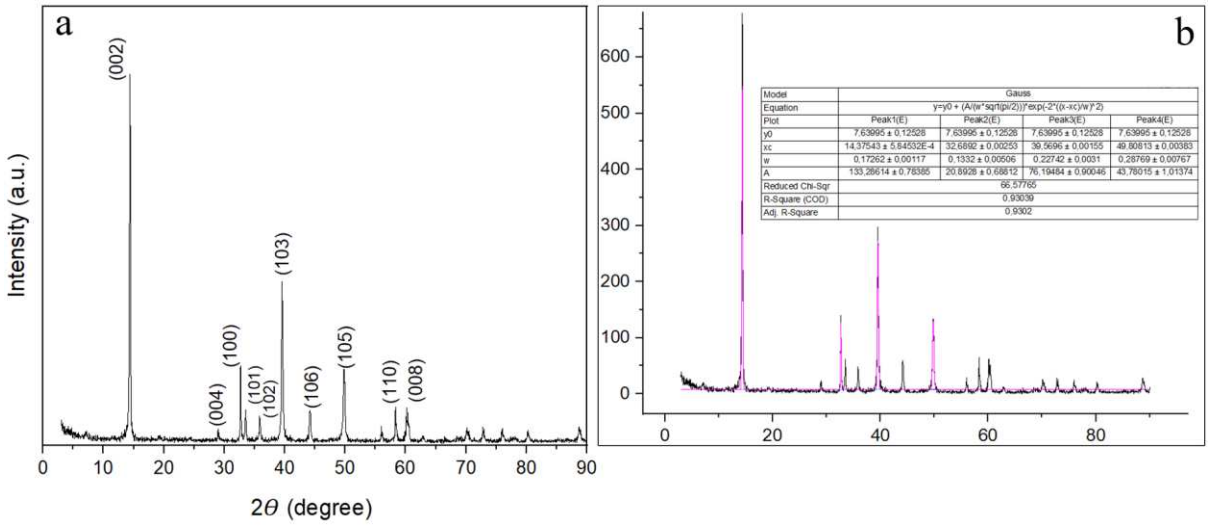


Fig. 6 MoS_2 a) XRD pattern b) Determination of FWHM and Bragg angles from XRD data.

Table 4 Determination of the size of the material whose peak position and FWHM value are determined according to XRD data, according to the Scherrer Equation.

Peak positions	FWHM	Crystallite Size D (nm)
14.3754	0.29324	27.96
32.6892	0.15683	60.18
39.5696	0.26776	38.48
49.80813	0.33873	36.34
Average Crystallite Size D (nm)		**40.74**

The discrepancy between the crystallite size determined by XRD (40.74 nm) and the particle size observed in SEM images (278–380 nm) is consistent with the polycrystalline nature of the MoS_2 particles, where each particle is composed of multiple crystalline domains.

3.1.4. XPS Analysis

The X-ray photoelectron spectroscopy (XPS) analysis was conducted to evaluate the chemical states and composition of the molybdenum (IV) sulfide (MoS_2) nanoparticles. The wide-scan XPS survey spectrum is presented in Fig. 7. The high-resolution XPS spectra of the Mo 3d and S 2p regions are shown in Fig. 8 and Fig. 9, respectively. The two characteristic peaks located around 229.07 eV and 232.5 eV correspond to the Mo 3d5/2 and Mo 3d3/2 orbitals, respectively [32]. Furthermore, the peaks belonging to sulfur, located at 162.13 eV and 163.1 eV, are clearly visible in the S 2p spectrum [33]. Detailed elemental identification and quantification data are provided in Table 5.

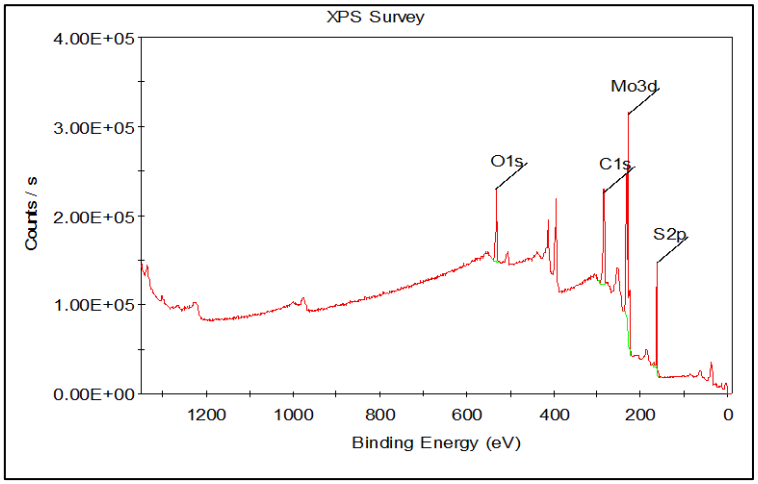


Fig. 7 XPS survey spectrum of MoS_2 nanoparticles

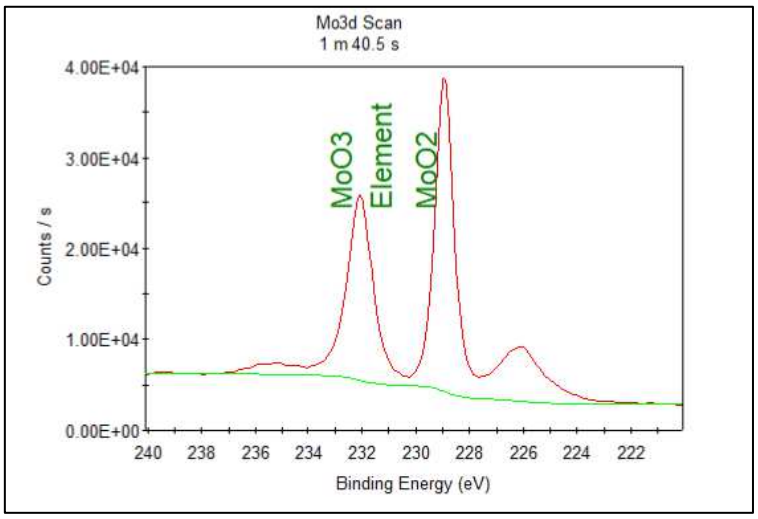


Fig. 8 XPS spectrum of the Mo 3d region.

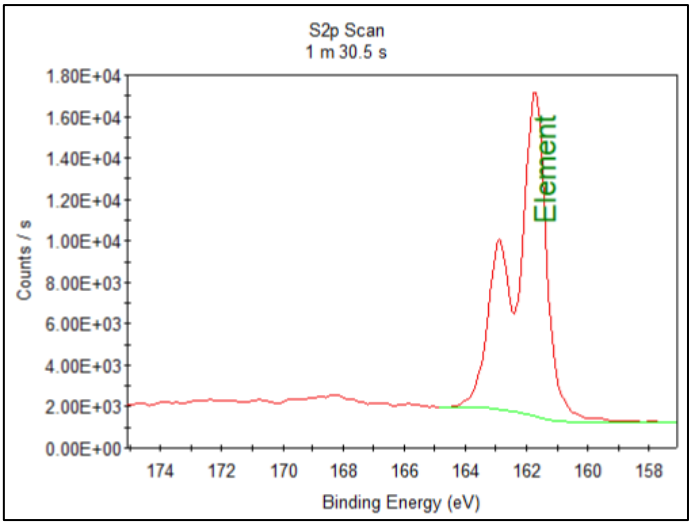


Fig. 9 XPS spectrum of the S 2p region.

Table 5 XPS elemental ID and quantification results of MoS_2

Name	Peak BE	FWHM eV	Area (P) CPS.eV	Weight %	Q
Mo3d	229.07	2.44	1014243.47	41.78	1
C1s	284.49	1.99	393572.07	23.13	1
O1s	532.10	3.62	327635.79	10.62	1
S2p	162.13	2.59	315987.59	24.46	1

Having confirmed the phase purity, crystallite size, and dispersion state of the nanoparticles, the machining performance of the five cooling/lubrication environments is evaluated next.

3.2. Surface roughness measurement results

Machining processes can achieve low surface roughness values, particularly when appropriate tooling, workpiece materials, and cutting conditions are employed [34]. It is well recognized that cooling/lubrication conditions significantly affect surface roughness [35]. Under the current experimental conditions, the effect of cooling/lubrication on surface roughness was investigated (Fig. 10a and Fig. 10b).

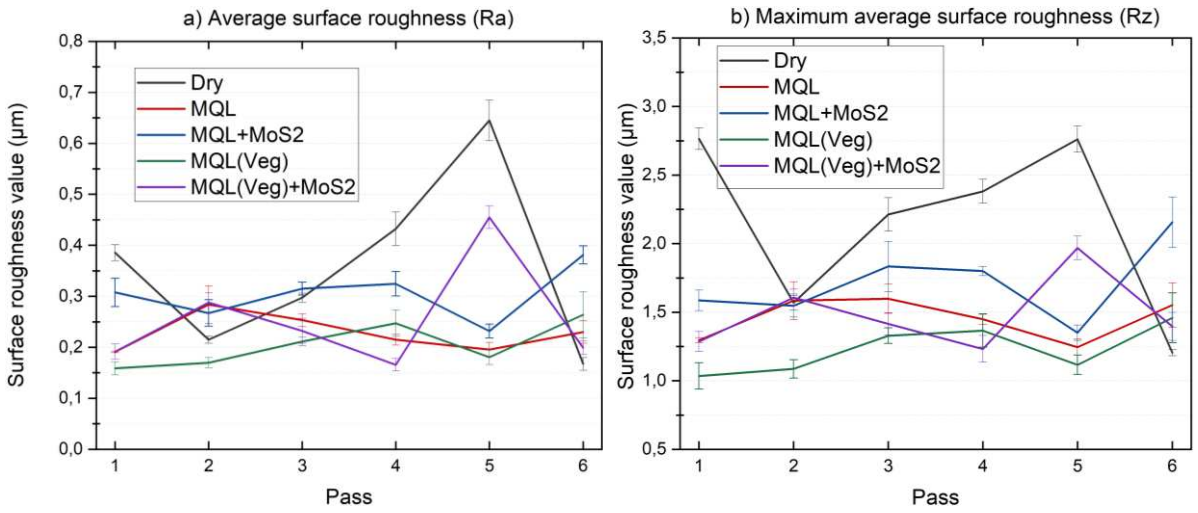


Fig. 10 Surface roughness values: **a)** Ra, **b)** Rz

The highest surface roughness (lowest surface quality) was achieved through dry cutting, as the absence of lubrication typically results in a poor surface finish [36]. The use of Minimum Quantity Lubrication (MQL) consistently resulted in better surface quality, regardless of the type of fluid used. For the employed feed per tooth ($f_z \approx 0.0094$ mm) and tool geometry, the kinematic (geometric) contribution to the surface profile is negligible, being on the order of 0.01 µm or less. As a result, the measured Ra values (0.159–0.645 µm) are governed almost entirely by tribological phenomena at the tool–workpiece interface, including adhesion, BUE formation and detachment, side flow, and micro-vibrations, rather than by feed marks. This explains the strong sensitivity of Ra to the cooling/lubrication environment shown in Fig. 10 and supports the interpretation that lubrication is the dominant surface-generation mechanism under the present machining conditions. Sunflower oil with MQL produced the best surface quality. However, the addition of MoS_2 nanoparticles had a limited effect, and the sunflower oil with MoS_2 nanoparticles showed no statistically significant improvement compared to the pure sunflower oil. This indicates that MoS_2 does not provide additional lubricity, as sunflower oil already possesses inherently superior lubricity. The lamellar structure of MoS_2 nanoparticles and their ability to form tribofilms under high contact pressure and boundary lubrication conditions should theoretically improve the surface; however, in this study, the already superior wetting properties of sunflower oil, which allowed it to effectively penetrate the shear zone, may have limited the contribution of MoS_2. Regarding average surface roughness (Ra), the poorest surface quality was observed under dry cutting conditions (Ra = 0.645 µm). Conversely, the most favorable results were achieved using MQL (Veg) (MQL with vegetable (sunflower) oil) and MQL (Veg) + MoS_2 with values of 0.159 µm and 0.166 µm, respectively. These findings demonstrate that the choice of cooling/lubrication medium significantly influences surface integrity. As anticipated, the Ra and Rz values exhibited similar trends. The Rz values were approximately four to six times higher than the Ra values across all experimental conditions. The higher Rz/Ra ratios observed under dry cutting are associated with isolated deep valleys and adhered-material peaks resulting from BUE detachment, while the lower ratios obtained under sunflower-oil MQL suggest a more homogeneous surface texture with fewer extreme asperities. A two-way ANOVA was performed to evaluate the effects of cooling/lubrication condition and pass number on the surface roughness (Ra) values (Table 6).

Table 6 ANOVA

Source	DF	Adj SS	Adj MS	F-Value	P-Value	η^2	Partial η^2
Conditions	4	0.4483	0.112081	62.11	0.000	0.244	0.674
Passes	5	0.1723	0.034460	19.10	0.000	0.094	0.443
Conditions*Passes	20	1.0009	0.050046	27.73	0.000	0.545	0.822
Error	120	0.2165	0.001804				
Total	149	1.8381					

The analysis revealed that both the cooling/lubrication condition ($F = 62.11$, $p < 0.001$) and pass number ($F = 19.10$, $p < 0.001$) had statistically significant effects on surface roughness (Table 6). More importantly, a highly significant interaction effect was observed between cooling/lubrication condition and pass number ($F = 27.73$, $p < 0.001$), indicating that the influence of the cooling/lubrication strategy on Ra was dependent on the pass number. The interaction sum of squares (SS = 1.0009) was considerably greater than those associated with the main effects of cooling/lubrication condition (SS = 0.4483) and pass number (SS = 0.1723), suggesting that the combined influence of these factors accounted for a substantial portion of the observed variability in surface roughness. In addition to statistical significance, effect size analysis revealed substantial contributions of all investigated factors. The cooling/lubrication condition, pass number, and their interaction yielded partial η^2 values of 0.674, 0.443, and 0.822, respectively, indicating large effect sizes. The interaction term exhibited the strongest influence on surface roughness, confirming that the effectiveness of the lubrication strategies changed considerably throughout the machining sequence.

The interaction plot further confirmed the statistical findings by exhibiting non-parallel response trends among the different pass levels across the cooling/lubrication conditions. The variation in the slope and direction of the profiles indicates that the effect of a given lubrication strategy changed throughout the machining sequence. In particular, certain lubrication conditions exhibited relatively stable Ra values over consecutive passes, whereas others showed pronounced fluctuations at specific pass numbers. Such behavior demonstrates that the effectiveness of the cooling/lubrication environments cannot be adequately evaluated independently of the pass number. Therefore, the significant interaction effect highlights the necessity of considering both factors simultaneously when assessing surface quality performance under different cooling/lubrication conditions. Accordingly, post-hoc multiple comparison tests were performed to identify the specific cooling/lubrication conditions that differed significantly within each pass level (Fig. 11).

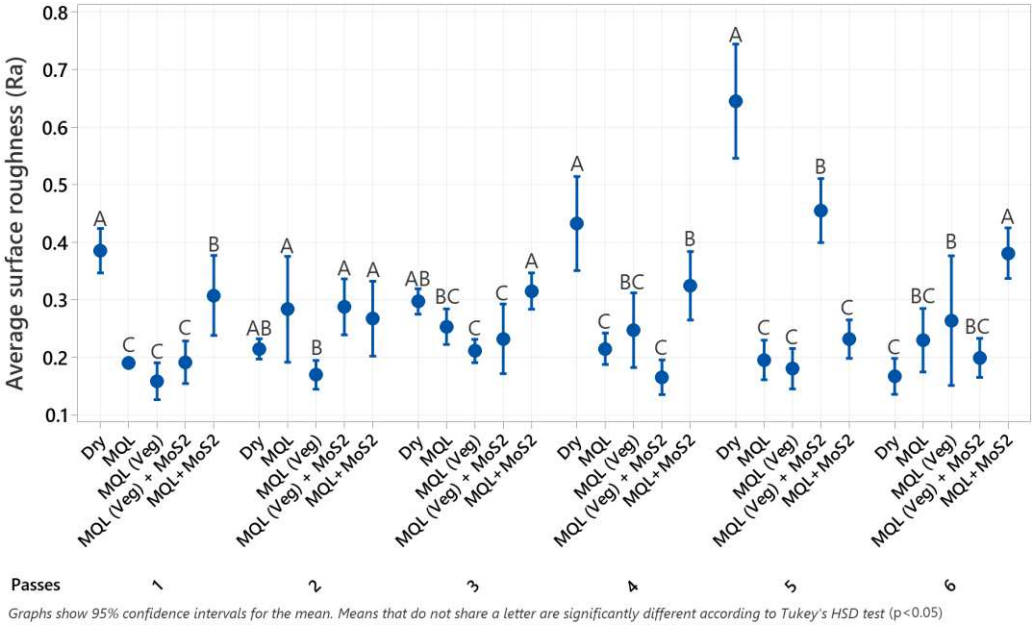


Fig. 11 Tukey HSD analysis

Fig. 11 presents the mean surface roughness (Ra) values and Tukey HSD grouping results for different cooling/lubrication conditions at each pass level. The results indicate that the effectiveness of the cooling/lubrication strategies varied considerably depending on the pass number, which is consistent with the significant interaction effect identified by the two-way ANOVA. In the first pass, the Dry condition produced the highest surface roughness and was significantly different from the MQL and MQL (Veg) conditions, while MQL+MoS_2 exhibited intermediate behavior. Similar trends were observed in the second and third passes, although the differences among some lubrication environments became less pronounced. In the fourth and fifth passes, the Dry condition yielded markedly higher Ra values and formed a distinct statistical group, whereas MoS_2-containing environments generally resulted in lower surface roughness values. The fifth pass exhibited the largest separation among the lubrication conditions, indicating that the influence of the lubrication strategy became more pronounced as machining progressed. In the sixth pass, MQL+MoS_2 produced significantly higher Ra values than the remaining lubrication conditions, while Dry, MQL, and MQL (Veg)+MoS_2 were grouped among the lowest roughness levels. The unexpectedly low Ra observed under dry cutting in the sixth pass can be attributed to the burnishing effect of the severely worn cutting edge. As flank wear flattens the cutting edge, the enlarged wear land plastically smears the newly generated surface, temporarily reducing Ra despite the deteriorated tool condition. This apparent improvement should therefore be interpreted as a consequence of tool degradation rather than an indication of improved cutting performance, further highlighting the importance of evaluating surface quality together with tool-wear evidence. Overall, the Tukey HSD results demonstrate that the relative performance of the cooling/lubrication environments changed throughout the machining sequence, confirming that surface roughness was governed by the combined effects of lubrication condition and pass number rather than by either factor alone. The statistical analysis demonstrated that lubrication conditions alone were insufficient to explain surface roughness evolution. The significant interaction effect indicates that the relative effectiveness of each lubrication strategy changed throughout the machining sequence as tool wear progressed.

3.3. Tool wear analysis

In a machining operation, tool wear is inevitable. To monitor tool wear progression, a toolmaker's microscope (Mahr MarVision MM200, Göttingen, Germany) was employed after each pass. The most severe tool wear occurred under dry machining conditions. Many studies have shown the negative impact of dry machining on tool wear [36, 37]. Wear was detected on all cutting edges beginning with the first pass. The wear values of 76 µm, 67 µm, 50 µm, and 90 µm were recorded for the four edges in the initial pass. In the last pass, 105 µm, 154 µm, 72 µm, and 252 µm of wear were measured. It was observed that one cutting edge exhibited accelerated wear in the second pass and continued to wear at a steady rate thereafter. This is a commonly reported tool wear pattern in the literature [38]. Fig. 12 shows measurements of the most-worn cutting edge under dry cutting conditions. The minor differences in the measurements can be attributed to BUE formation and measurement variability. The remaining three cutting edges exhibited minimal and approximately linear wear.

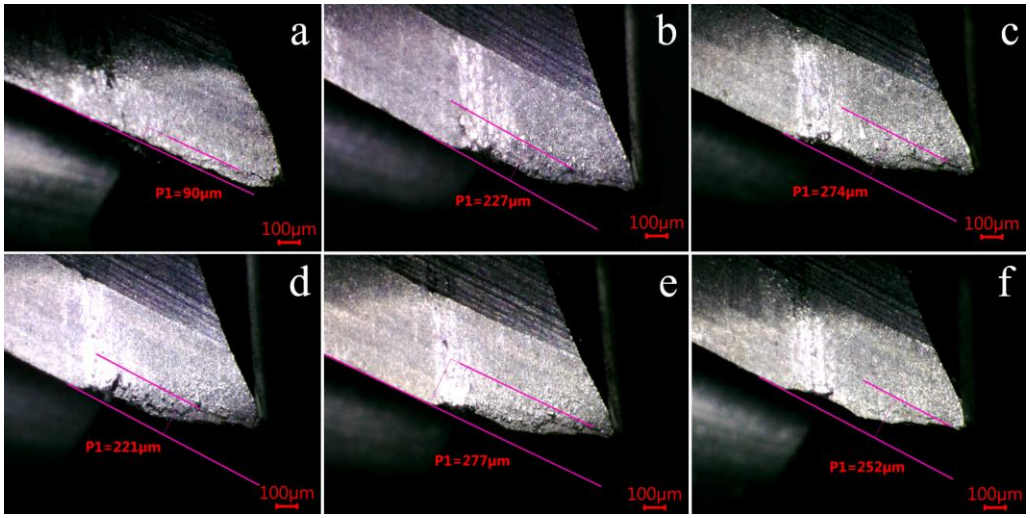


Fig. 12 The toolmaker's microscope inspection, first run (a) to sixth run (f)

Under the lubrication-assisted conditions, flank wear (VB) remained below the resolution limit of the optical measurement system and therefore could not be quantified reliably. Consequently, SEM and EDX analyses were employed to compare the dominant wear mechanisms and coating integrity among the investigated lubrication environments. Therefore, detailed scanning electron microscope (SEM) and energy-dispersive X-ray spectroscopy (EDX) examinations were performed upon completion of the experiments. All cutting tools were examined using a ZEISS GeminiSEM 500 (Carl Zeiss, Jena, Germany) to evaluate the impact of the five cooling/lubrication strategies on tool wear mechanisms.

3.4. SEM-EDX analysis and results of cutting tools

The SEM and EDX analyses focused on the cutting tool used under dry machining. Elemental composition was determined at specific locations designated as Spot 1 and Areas 1–3 (Fig. 13).

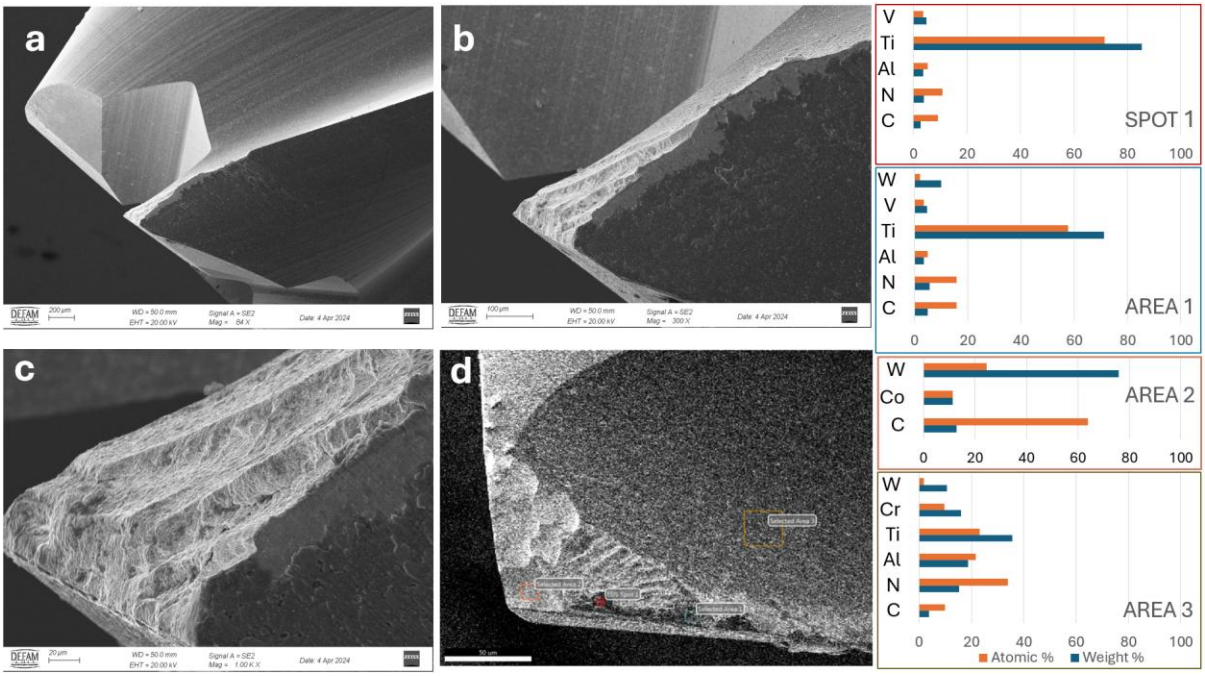


Fig. 13 SEM image of the cutting tool used in dry machining conditions. a)84×, b) 300×, c)1000× and d) EDX image

Fig. 13 clearly shows that the cutting corner was fractured, and the cutting tool's coating had delaminated. The tool's substrate was visible at the corner. In EDX analysis, high concentrations of titanium (Ti), aluminum (Al), and vanadium (V), which are the primary alloying elements of the workpiece (Ti6Al4V ELI), confirm BUE formation in both Spot 1 and Area 1. The detection of only tungsten (W), carbon (C), and cobalt (Co) in Area 2 indicates a worn/lost coating in this region and reveals the WC-Co substrate. Cutting tool coatings significantly enhance tool performance, especially the tool life [39]. The absence of a protective coating layer leads to accelerated tool wear [40].

Analysis of Area 3 revealed limited titanium, indicating minimal material adhesion rather than significant BUE formation. Compared to some examples in the literature, BUE formation in this study appears limited [41]. Additionally, elements from both the coating (AlCrN) and the substrate were detected in this area. These findings demonstrate severe fractures on the cutting edge and wear on the coating under dry machining. The tool used under MQL conditions was subsequently subjected to EDX analysis (Fig. 14).

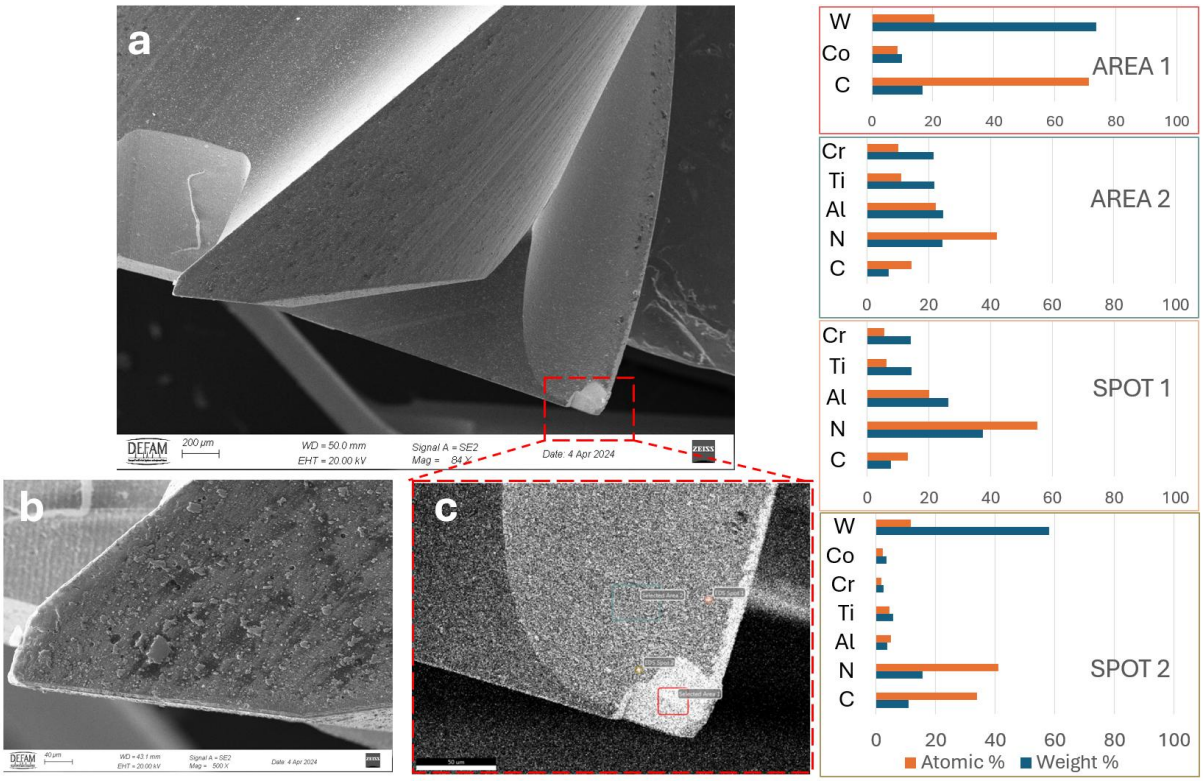


Fig. 14 SEM image of the cutting tool used under MQL machining conditions, a)84×, b) 500×, and c) EDX image

MQL conditions resulted in a change in tool wear behavior. A corner fracture was also observed under MQL conditions; however, compared to dry cutting, the fracture was less severe, and the wear was more concentrated on the rake face. Fig. 8 clearly exhibits coating delamination on the rake surface. The EDX analysis of Area 1 revealed the presence of only tungsten (W), carbon (C), and cobalt (Co), indicating that the surface corresponds entirely to the cutting tool substrate. The observed wear is more fracture-like rather than the typical crater wear reported in the literature [42]. In Area 2, elements associated with the AlCrN coating, as well as a small amount of titanium, were detected. This is attributed to BUE formation. Similar results were observed for spots 1 and 2. However, the presence of tungsten in spot 2 indicates partial coating loss and substrate exposure. Fig. 15 presents SEM images of the cutting tool used during the machining of Ti6Al4V ELI under nanoparticle-enhanced (MoS_2) MQL conditions.

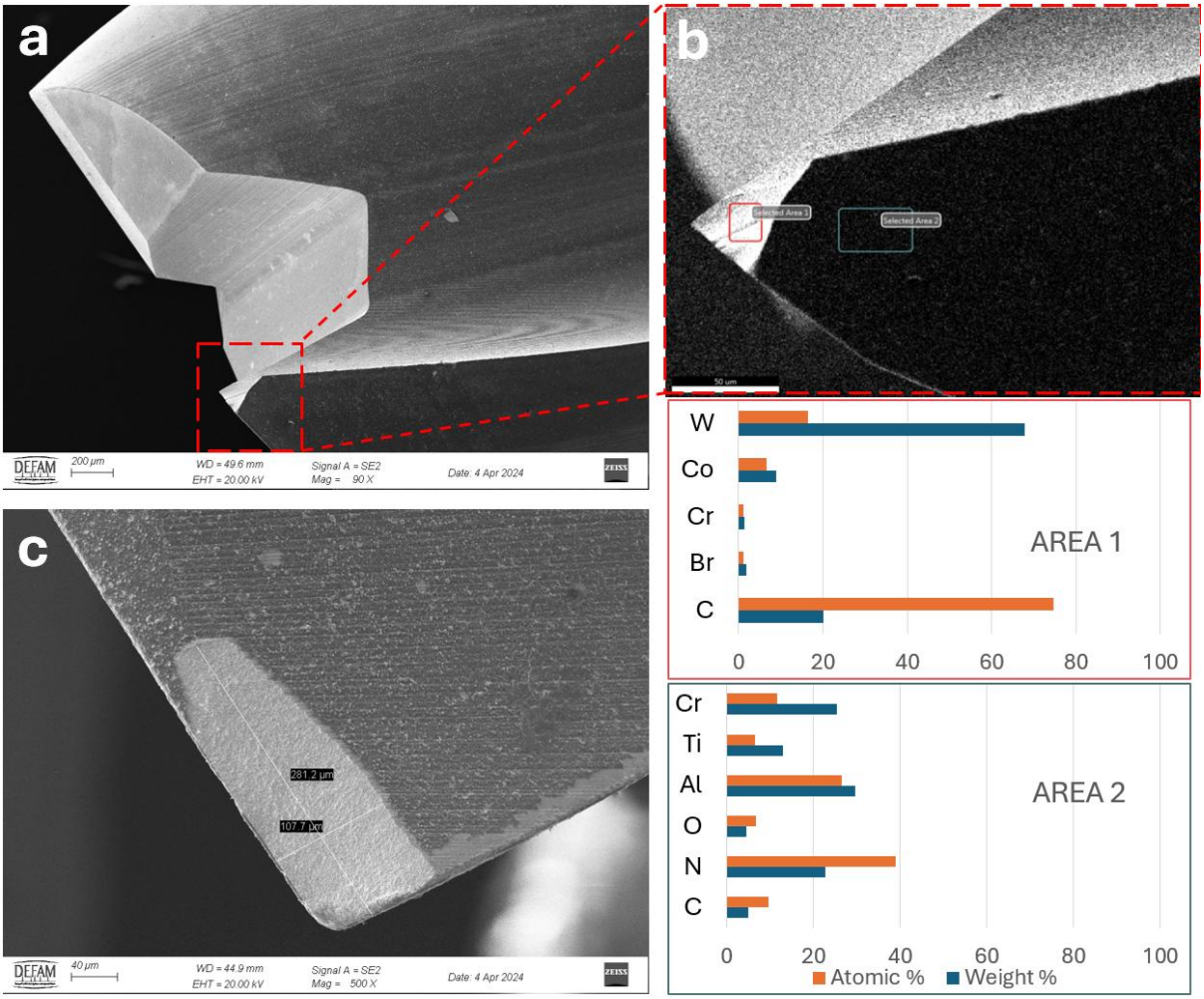


Fig. 15 SEM image of the cutting tool used under nanoparticle-enhanced cutting fluid MQL, a) 90×, b) EDX image, and c) 500×

In the examination of MQL with MoS_2, a significant fracture on the cutting edge was detected, but the size of the fracture was found to be smaller compared to dry and standard MQL machining conditions (Fig. 15). This type of fracture was not observed on the other cutting edges. This indicates that the MoS_2 additive contributes to reduced tool wear and has a positive effect on tool life. According to EDX analysis, the fractured surface contained mostly tungsten (W), carbon (C), and cobalt (Co), while a small amount of chromium (Cr) was associated with the tool coating. The Beryllium element detected in the analysis could not be directly associated with the workpiece or the cutting tool; this indication is likely an artifact arising from spectral overlaps in the EDX measurement rather than physical contamination. It was determined that the tool coating contained mostly AlCrN, while the limited amount of titanium (Ti) could be explained by BUE. In addition, examinations of the rake face of the other cutting edge (Fig. 9c) indicate that the coating layer (AlCrN) reacted with the workpiece material (Ti6Al4V ELI). This chemical interaction led to rapid wear, revealing crater wear in an area of approximately 108 µm x 281 µm. Crater wear is a typical type of failure encountered during the machining of Ti6Al4V [43]. However, the crater wear dimensions observed in this study are notably higher (around two to three times) compared to the literature [44, 45]. This phenomenon can be attributed to the severe thermal conditions generated during the 84-minute prolonged machining protocol. Although the MoS_2-enhanced MQL system

provides superior boundary lubrication, its convective cooling capacity is inherently lower than that of conventional flood cooling. Coupled with the extremely low thermal conductivity of the Ti6Al4V ELI alloy, intense heat remains highly localized at the tool-chip interface. These sustained high-temperature conditions accelerate the chemical affinity and diffusion mechanisms between the AlCrN coating and the titanium workpiece, ultimately promoting the expansion of the crater wear. These observations suggest that the beneficial effect of MoS_2 is mechanism specific. The nanoparticles effectively reduce adhesion-driven mechanical damage, such as BUE formation and edge chipping; however, they are unable to suppress the thermally activated diffusion–dissolution wear responsible for crater formation at the tool–chip interface. This difference explains why MoS_2 improved edge integrity, while the crater dimensions remained relatively large under the prolonged machining conditions. Fig. 16 shows SEM analyses of MQL machining of Ti6Al4V ELI using sunflower oil.

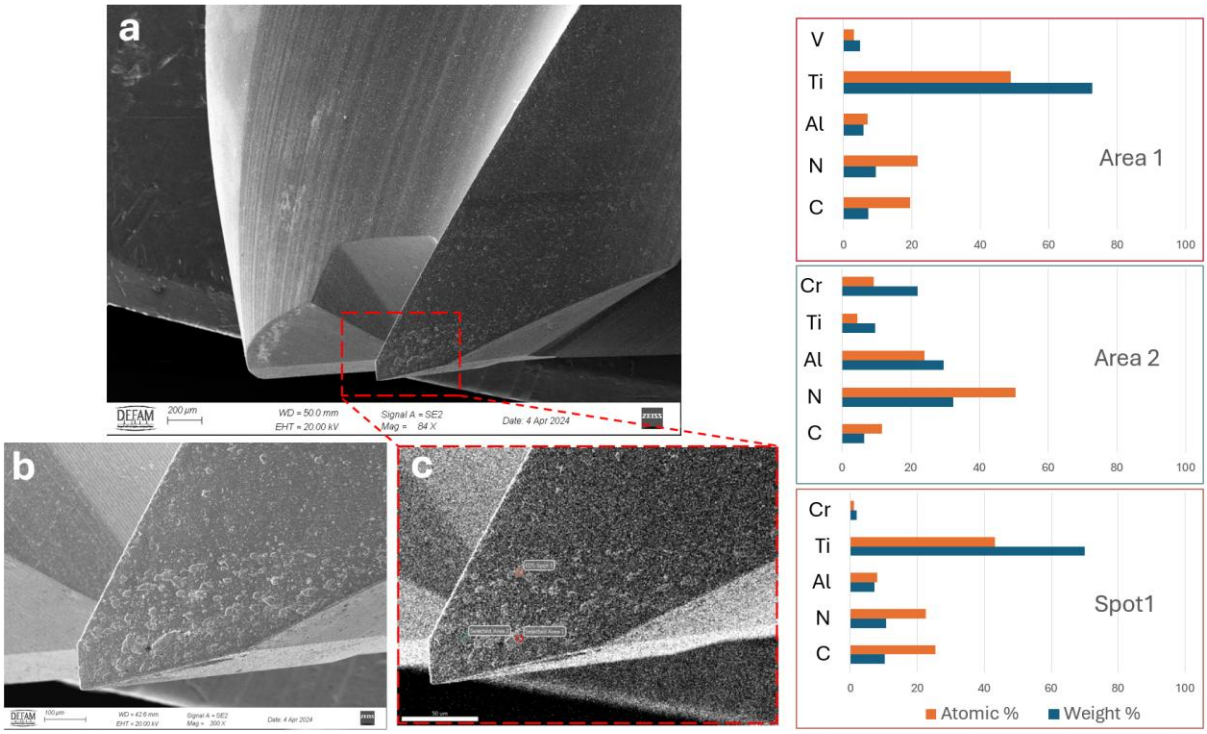


Fig. 16 SEM image of the cutting tool used in MQL machining conditions with sunflower oil, a) 84×, b) 300×, and c) EDX image

The SEM observations indicate that sunflower oil provides favorable tribological performance under MQL conditions. Sunflower oil has been reported to exhibit excellent wettability and lubrication characteristics, which contribute to reduced friction, lower cutting forces, and improved surface quality [46]. In addition to wettability, the boundary-lubrication performance of sunflower oil is strongly promoted by its triglyceride structure: the polar ester groups and long unsaturated fatty-acid chains (predominantly oleic and linoleic acids) adsorb onto freshly generated metal surfaces and form a durable boundary film, while its higher viscosity (65.2 cSt vs. 18 cSt, Table 3) further stabilizes this film under the high contact pressures of the cutting zone.

The fracture observed under other cutting conditions was not present in this case. However, significant material adhesion was detected on the tool surface. EDX analyses revealed that the chemical composition in Area 1 included titanium, aluminum, and vanadium, indicating BUE formation. In contrast, Area 2 showed a chemical composition associated with the cutting tool coating (AlCrN), with only trace amounts of titanium related to BUE. Similar conclusions can be drawn for Spot 1, although the percentages may vary. These findings demonstrate the positive effects and high performance of MQL machining with sunflower oil on the cutting tool. The inspection of nano-particle additives in sunflower oil using MQL application is presented in Fig. 17.

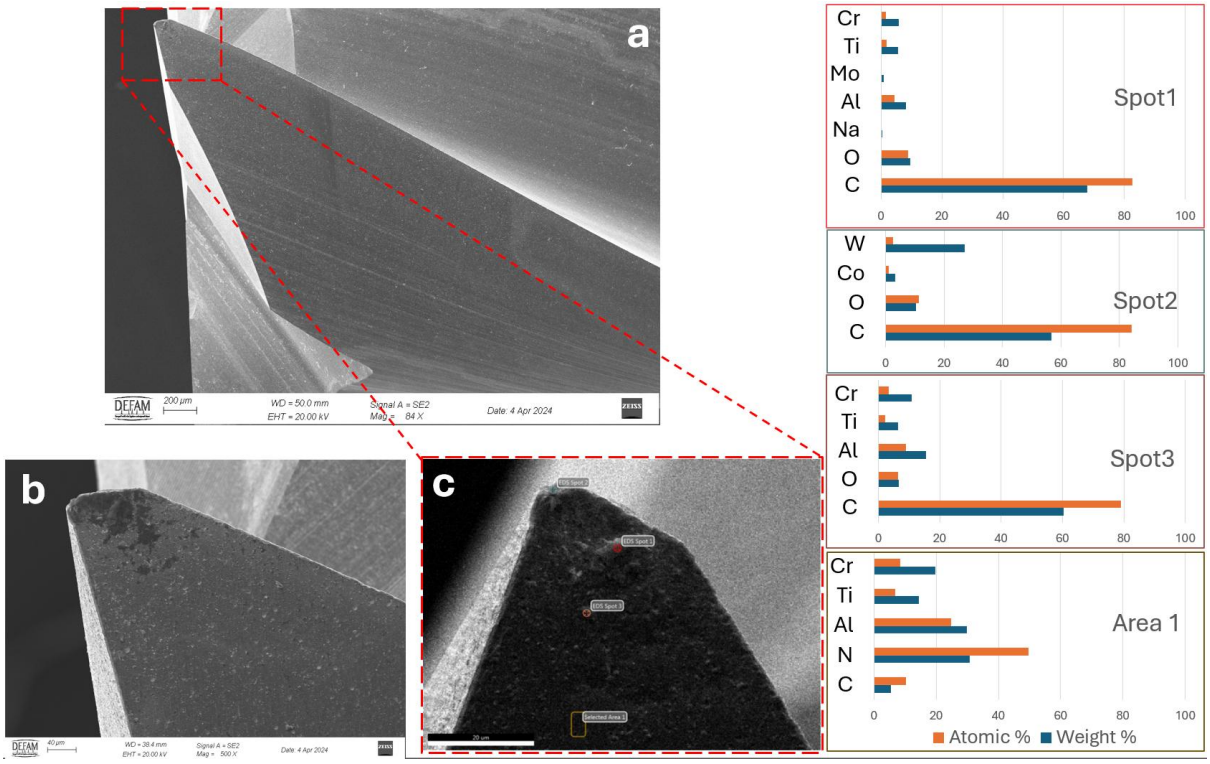


Fig. 17 SEM image of the cutting tool used in MQL machining conditions using nanoparticle-reinforced sunflower oil, a) 84×, b) 500×, and c) EDX image

Similar to the previous sunflower oil MQL application, no fracture was observed on the cutting edge in the SEM analysis. MQL applications using sunflower oil and nanoparticles can also produce favorable results. EDX analysis of both Area 1 and Spot 1 revealed that the elemental composition was primarily composed of the cutting tool coating (AlCrN), with trace amounts of titanium related to minor BUE formation. Additionally, the presence of oxygen may be associated with oxidation or contamination. Among all MQL strategies, sunflower oil-based MQL yielded superior surface integrity; the further incorporation of MoS_2 nanoparticles into sunflower oil provided additional tribological benefits, particularly in terms of tool wear suppression.

The improved performance observed under MoS_2-enhanced MQL can be attributed to the solid lubrication characteristics of MoS_2 nanoparticles, particularly under boundary lubrication conditions. During the machining of Ti6Al4V ELI, the lubricant film can become unstable due to high thermomechanical loads. In such cases, the layered structure of MoS_2 allows easy shear between its atomic planes, which helps reduce friction at the tool–chip interface [47, 48].

In addition, the small size of the particles enables them to reach the cutting zone and form a thin tribological layer on the tool surface. This layer likely limits direct metal-to-metal contact. SEM observations show reduced built-up edge (BUE) formation and less coating damage compared to dry and conventional MQL conditions. The EDX results also suggest reduced material adhesion, supporting the idea that MoS_2 contributes to improved wear behavior.

Although the incorporation of MoS_2 nanoparticles did not result in a statistically significant improvement in surface roughness compared with sunflower-oil-based MQL, SEM observations suggest a beneficial influence on tool wear behavior. Surface roughness in milling operations is primarily governed by tool geometry, tool runout, feed marks, vibration, and the lubrication conditions directly affecting the freshly generated surface. Since sunflower oil already possesses excellent wettability and boundary lubrication characteristics, the addition of MoS_2 provided limited additional benefit in terms of surface finish. In contrast, tool wear is a cumulative phenomenon that develops progressively under repeated thermo-mechanical loading. The layered crystal structure of MoS_2 can reduce friction at the tool–chip interface and help maintain a more stable lubricating environment during prolonged machining. Consequently, the contribution of MoS_2 appears to be more pronounced in suppressing coating damage, material adhesion, and localized edge degradation rather than in further reducing surface roughness. These findings indicate that the primary benefit of MoS_2 under the present machining conditions is associated with improved tool preservation rather than additional enhancement of surface quality.

Limitations and Future Work

Despite these positive outcomes, the present study is limited to a constant set of cutting parameters (Vc = 100 m/min, f = 300 mm/min), a single MoS_2 nanoparticle concentration (0.5 vol.%) and a single prolonged run per lubrication condition. Additionally, direct sustainability metrics such as specific energy consumption and carbon emissions were not quantified. Future research should focus on evaluating a broader range of machining parameters, varying nanoparticle concentrations, and optimizing MQL flow rates. Furthermore, a detailed investigation of chip morphology and a comprehensive Life Cycle Assessment (LCA) will be conducted to fully evaluate the environmental and economic impacts of this sustainable machining approach.

4. Conclusions

This study evaluated the influence of dry, conventional MQL, MoS_2-reinforced MQL, sunflower-oil-based MQL, and MoS_2-reinforced sunflower-oil-based MQL environments on the machinability of Ti6Al4V ELI (Grade 23). Based on the experimental findings, the main conclusions are summarized as follows:

1. Dry machining is impractical for Ti6Al4V ELI due to severe thermal loads that lead to edge fractures and extensive coating delamination. The integration of MQL strategies significantly enhanced surface quality, improving surface roughness (Ra) by up to 75% compared to dry cutting (from 0.645 μm to 0.159 μm).

2. Vegetable (sunflower) oil-based MQL outperformed general-purpose cutting fluid alternatives due to its superior wetting characteristics, yielding the lowest surface roughness values. However, a significant interaction effect between the lubrication condition and the pass number indicates that the surface roughness evolution is time-dependent and progressive tool wear modifies the effectiveness of each strategy across consecutive passes.
3. The addition of 0.5 vol.% MoS_2 nanoparticles effectively suppressed built-up edge (BUE) formation. Although MoS_2 did not significantly improve surface roughness, SEM observations suggest that it contributed primarily to wear suppression rather than surface finish enhancement. SEM-EDX analyses suggested the formation of a tribological layer attributed to MoS_2, which reduced direct metal-to-metal contact, material adhesion, and coating damage. MoS_2 demonstrated enhanced lubrication stability at higher pass counts, suggesting its effectiveness in maintaining tool integrity under increasing cumulative thermal stress.

4. Sunflower-oil-based MQL aligns with modern sustainable machining standards, offering a clean, non-toxic, and viable alternative to conventional flood cooling in precision manufacturing applications.

5. Material characterization confirmed the chemical and structural integrity of the commercial MoS_2 nanoparticles. XRD analysis verified the hexagonal MoS_2 phase with a mean crystallite size of 40.74 nm — consistent with the polycrystalline nature of the particles observed in SEM images (200–400 nm range) without significant agglomeration. FTIR and XPS analyses successfully verified the characteristic Mo–S bonds and indicated no significant oxide phase formation.

6. For practical applications, sunflower-oil MQL at 150 ml/h can be considered a sustainable alternative to commercial cutting fluids for the finish milling of Ti6Al4V ELI. The addition of 0.5 vol.% MoS_2 may be beneficial when tool life, rather than surface finish, is the primary production constraint.

Acknowledgments
This study was supported by the Manisa Celal Bayar University Scientific Research Projects Coordination Unit. Project Number: 2023-028. During the preparation of this work the authors used Google Gemini for English language editing. After using this tool/service, the authors reviewed and edited the content as needed and took full responsibility for the content of the published article.

Author contributions Deniz ÇOBAN ÖZKAN: Conceptualization, Data curation, Formal analysis, Funding acquisition, Investigation, Methodology, Project administration, Resources, Validation, Visualization, Writing – original draft, Writing – review and editing. Fikret SÖNMEZ: Conceptualization, Data curation, Formal analysis, Funding acquisition, Investigation, Methodology, Resources, Validation, Visualization, Writing – original draft, Writing – review and editing.

Declarations
Conflict of interest We declare that we have no financial and personal relationships with other people or organizations that can inappropriately influence our work, there is no professional or other personal intersest of

any nature or kind in any product, service and/or company that could be construed as influencing the position presented in, or the review of, the manuscript entitled. All the authors have been involved with the work agree to submit this paper to Arabian Journal for Science and Engineering, and all authors claim that none of the material in the paper has been published or is under consideration for publication elsewhere.

Data availability

The datasets generated and analyzed during the current study are available from the corresponding author on reasonable request.

References

1. Liao Z, Schoop JM, Saelzer J, Bergmann B, Priarone PC, Splettstößer A. Review of current best-practices in machinability evaluation and understanding for improving machining performance. CIRP Journal of Manufacturing Science and Technology. 2024;50:151-84. https://doi.org/10.1016/j.cirpj.2024.02.008
2. Podulka P, Felho C, Sztankovics I, Knapčíková L. Roughness evaluation of machined Ti-6Al-4V alloys with a study of surface topography measurement noise. Measurement. 2026;257. https://doi.org/10.1016/j.measurement.2025.118686
3. Ruzova TA, Haddadi B. Surface roughness and its measurement methods - Analytical review. Results in Surfaces and Interfaces. 2025;19. https://doi.org/10.1016/j.rsurfi.2025.100441
4. Shetty RP, Marakini V, D'Mello G, P SP. Surface roughness modeling and prediction in high speed turning of Ti6Al4V alloy using artificial neural networks. Progress in Engineering Science. 2025;2. https://doi.org/10.1016/j.pes.2025.100146
5. Xu N, Wang D, Taylor C, Secker J, de Boer G, Thompson H, et al. Adhesive layer formation and its dual role in tribological performance and surface integrity of Ti-6Al-4V: Implications for the machining process. Tribology International. 2026;214. https://doi.org/10.1016/j.triboint.2025.111228
6. He T, Liu N, Xia H, Wu L, Zhang Y, Li D. Progress and trend of minimum quantity lubrication (MQL): A comprehensive review. Journal of Cleaner Production. 2023;386. https://doi.org/10.1016/j.jclepro.2022.135809
7. Hukkerikar AV, Arrazola PJ, Aristimuño P, Norgren S, Morandeau A, Joly D. A tribological characterisation of Ti-48Al-2Cr-2Nb and Ti-6Al-4V alloys with dry, flood, and MQL lubricants. CIRP Journal of Manufacturing Science and Technology. 2023;41:501-23. https://doi.org/10.1016/j.cirpj.2022.11.016
8. Prakash T, Arun A, Sachin A. Investigation of non-edible vegetable oil as cutting fluid in boring operation using MQL technique for CEW-1 steel. Materials Today: Proceedings. 2023;72:1462-6. https://doi.org/10.1016/j.matpr.2022.09.346
9. Saha S, Deb S, Bandyopadhyay PP. Tool wear induced burr formation and concomitant reduction in MQL wetting capability in micro-milling. International Journal of Mechanical Sciences. 2023;245. https://doi.org/10.1016/j.ijmecsci.2022.108095
10. Groover MP. Fundamentals of Modern Manufacturing: Materials, Processes and Systems. USA: John Wiley & Sons; 2010.
11. Callister WD, Rethwisch DG. Materials Science and Engineering: An Introduction. Wiley; 2013.
12. Sarma D, Ozah R, Chandrasekaran M, Sahoo AK, Kumar R, Pattanayak S. Material-specific machining optimization of Ti6Al4V alloy under MQL: A sustainability-centric approach. Next Materials. 2025;8. https://doi.org/10.1016/j.nxmate.2025.100586
13. Ni C, Wang X, Zhu L, Liu D, Wang Y, Zheng Z. Machining performance and wear mechanism of PVD TiAlN/AlCrN coated carbide tool in precision machining of selective laser melted Ti6Al4V alloys under dry and MQL conditions. Journal of Manufacturing Processes. 2022;79:975-89. https://doi.org/10.1016/j.jmapro.2022.05.036
14. Swain S, Kumar R, Panigrahi I, Sahoo AK, Panda A. Machinability performance investigation in CNC turning of Ti–6Al–4V alloy: Dry versus iron-aluminium oil coupled MQL machining comparison.

International Journal of Lightweight Materials and Manufacture. 2022;5:496-509. https://doi.org/10.1016/j.ijlmm.2022.06.002
15. Yücel A, Yıldırım Ç V, Sarıkaya M, Şirin Ş, Kıvak T, Gupta MK. Influence of MoS2 based nanofluid-MQL on tribological and machining characteristics in turning of AA 2024 T3 aluminum alloy. Journal of Materials Research and Technology. 2021;15:1688-704. https://doi.org/10.1016/j.jmrt.2021.09.007
16. Sahoo SP, Datta S. Dry, MQL, and Nanofluid MQL Machining of Ti–6Al–4V Using Uncoated WC–Co Insert: Application of Jatropha Oil as Base Cutting Fluid and Graphene Nanoplatelets as Additives. Arabian Journal for Science and Engineering. 2020;45:9599-618. https://doi.org/10.1007/s13369-020-04849-0
17. Sen B, Gupta MK, Mia M, Mandal UK, Mondal SP. Wear behaviour of TiAlN coated solid carbide end-mill under alumina enriched minimum quantity palm oil-based lubricating condition. Tribology International. 2020;148. https://doi.org/10.1016/j.triboint.2020.106310
18. Jyothish P, Vasu V, Kashinath D. Experimental investigation study on enhancing the thermal and rheological properties of sunflower vegetable oil with ZnTiO3, BN, CuO nanofluid for machining of Inconel-718 under minimum quantity lubrication (MQL). Materials Today: Proceedings. 2022;59:1599-607. https://doi.org/10.1016/j.matpr.2022.03.147
19. Junankar AA, Parate SR, Dethe PK, Dhote NR, Gadkar DG, Gadkar DD. Optimization of bearing steel turning parameters under CuO and ZnO nanofluid-MQL using MCDM hybrid approach. Materials Today: Proceedings. 2021;47:4292-7. https://doi.org/10.1016/j.matpr.2021.04.589
20. Azami A, Salahshournejad Z, Shakouri E, Sharifi AR, Saraeian P. Influence of nano-minimum quantity lubrication with MoS2 and CuO nanoparticles on cutting forces and surface roughness during grinding of AISI D2 steel. Journal of Manufacturing Processes. 2023;87:209-20. https://doi.org/10.1016/j.jmapro.2023.01.029
21. Gnanavel C, Saravanan R, Baskaran P, Vignesh M, Aneesh VN, Anbuchezhiyan G. Tool wear effects on green and WCO/MoS2 nanofluid clean machining. Materials Today: Proceedings. 2023. https://doi.org/10.1016/j.matpr.2023.03.279
22. Makhesana MA, Patel KM, Krolczyk GM, Danish M, Singla AK, Khanna N. Influence of MoS2 and graphite-reinforced nanofluid-MQL on surface roughness, tool wear, cutting temperature and microhardness in machining of Inconel 625. CIRP Journal of Manufacturing Science and Technology. 2023;41:225-38. https://doi.org/10.1016/j.cirpj.2022.12.015
23. Çamlı KY, Demirsöz R, Boy M, Korkmaz ME, Yaşar N, Giasin K. Performance of MQL and Nano-MQL Lubrication in Machining ER7 Steel for Train Wheel Applications. Lubricants. 2022;10(4):48. https://doi.org/10.3390/lubricants10040048
24. Günan F, Kıvak T, Yıldırım Ç V, Sarıkaya M. Performance evaluation of MQL with AL2O3 mixed nanofluids prepared at different concentrations in milling of Hastelloy C276 alloy. Journal of Materials Research and Technology. 2020;9:10386-400. https://doi.org/10.1016/j.jmrt.2020.07.018
25. Tadi KK, Narayanan TN, Arepalli S, Banerjee K, Viswanathan S, Liepmann D. Engineered 2D nanomaterials-protein interfaces for efficient sensors. Journal of Materials Research. 2015;30:3565-74. https://doi.org/10.1557/jmr.2015.349
26. Ali GAM, Thalji MR, Soh WC, Algarni H, Chong KF. One-step electrochemical synthesis of MoS2/graphene composite for supercapacitor application. Journal of Solid State Electrochemistry. 2020;24:25-34. https://doi.org/10.1007/s10008-019-04449-5
27. Jiang Y, Wang J, Wu J, Zhang Y. Preparation of high-performance natural rubber/carbon black/molybdenum disulfide composite by using the premixture of epoxidized natural rubber and cysteine-modified molybdenum disulfide. Polymer Bulletin. 2021;78:1213-30. https://doi.org/10.1007/s00289-020-03157-9
28. Govindasamy M, Wang SF, Alothman AA, Alshgari RA, Ganesh PS. Synergetic effect of the ultrasonic-assisted hydrothermal process on the photocatalytic performance of MoS2 and WS2 nanoparticles. Journal of Materials Science: Materials in Electronics. 2022;33:8858-67. https://doi.org/10.1007/s10854-021-06934-y
29. Kamli K, Hadef Z. Binary Semiconductors Thin Films Characterization for Solar Cells Applications. Thin Films Photovoltaics. IntechOpen; 2022 https://doi.org/10.5772/intechopen.100513.

30. Langford J, Wilson A. Scherrer after Sixty Years: A Survey and Some New Results in the Determination of Crystallite Size. Journal of Applied Crystallography. 1978;11:102-13. https://doi.org/10.1107/S0021889878012844
31. Monshi A, Foroughi MR, Monshi MR. Modified Scherrer equation to estimate more accurately nano-crystallite size using XRD. World Journal of Nano Science and Engineering. 2012;2:154-60. https://doi.org/10.4236/wjnse.2012.23020
32. Yun J, Noh Y, Lee C, Na S, Lee S, Jo SM. Exfoliated and Partially Oxidized MoS2 Nanosheets by One-Pot Reaction for Efficient and Stable Organic Solar Cells. Small. 2014;10:2319-24. https://doi.org/10.1002/smll.201303648
33. Lamkaouane H, Ftouhi H, Richard-Plouet M, Gautier N, Stephant N, Zazoui M. Efficient and Facile Synthetic Route of MoO3:MoS2 Hybrid Thin Layer via Oxidative Reaction of MoS2 Nanoflakes. Nanomaterials. 2022;12(18):3171. https://doi.org/10.3390/nano12183171
34. Kaymak B, Öztürk F. Investigating the influence of machining parameters and tool coatings on surface quality of titanium parts in aerospace industry. NOHU Journal of Engineering Sciences. 2025;14:27-35. https://doi.org/10.28948/ngmuh.1525630
35. Pimenov DY, da Silva LRR, Machado AR, França PHP, Pintaude G, Unune DR. A comprehensive review of machinability of difficult-to-machine alloys with advanced lubricating and cooling techniques. Tribology International. 2024;196. https://doi.org/10.1016/j.triboint.2024.109677
36. Zhang Z, Deng J, Lu Y, Tang X, Bao Y. Dry cutting performance and mechanism of tools with textured composite coatings fabricated by EHDA. Journal of Manufacturing Processes. 2025;156:365-80. https://doi.org/10.1016/j.jmapro.2025.11.063
37. He Q, DePaiva JM, Kohlscheen J, Veldhuis SC. Analysis of the performance of PVD AlTiN coating with five different Al/Ti ratios during the high-speed turning of stainless steel 304 under dry and wet cooling conditions. Wear. 2022;492-493. https://doi.org/10.1016/j.wear.2021.204213
38. Sujay BJ, Anand Singh S, Agarwal A, Desai KA, Mears L. Identifying Tool Wear Stages in Turning Process through Machined Surface Image Analysis Using Convolutional Neural Network. Manufacturing Letters. 2025;44. https://doi.org/10.1016/j.mfglet.2025.06.079
39. Lin G, Shi H, Liu X, Wang Z, Zhang H, Zhang J. Tool wear on machining of difficult-to-machine materials: a review. International Journal of Advanced Manufacturing Technology. 2024;134:989-1014. https://doi.org/10.1007/s00170-024-14193-4
40. Sousa VFC, Castanheira J, Silva FJG, Fecheira JS, Pinto G, Baptista A. Wear behavior of uncoated and coated tools in milling operations of ampco (Cu-be) alloy. Applied Sciences. 2021;11. https://doi.org/10.3390/app11167762
41. Chowdhury MSI, Bose B, Rawal S, Fox-Rabinovich GS, Veldhuis SC. Investigation of the wear behavior of pvd coated carbide tools during ti6al4v machining with intensive built up edge formation. Coatings. 2021;11:1-17. https://doi.org/10.3390/coatings11030266
42. Hussein R, Sadek A, Elbestawi MA, Helmi Attia M. The effect of mql on tool wear progression in low-frequency vibration-assisted drilling of cfrp/ti6al4v stack material. Journal of Manufacturing and Materials Processing. 2021;5. https://doi.org/10.3390/jmmp5020050
43. Zhuang K, Li M, Lin F, Hu C, Weng J, Gao Z. Crater wear prediction in turning Ti6Al4V considering cutting temperature effect. The International Journal of Advanced Manufacturing Technology. 2022;121(9):6763-81. https://doi.org/10.21203/rs.3.rs-1414352/v1
44. Fang W, Chen J, Cai F, Zhou Q, Li M, Zhang S. Reduced crater wear and improved high-speed dry cutting performance of B-containing AlTiBN coatings against Ti-6Al-4 V alloy. Tribology International. 2023;187. https://doi.org/10.1016/j.triboint.2023.108730
45. Maruda RW, Szczotkarz N, Michalski M, Arkusz K, Wojciechowski S, Niesłony P. Evaluation of tool wear during turning of Ti6Al4V alloy applying MQL technique with Cu nanoparticles diversified in terms of size. Wear. 2023;532-533. https://doi.org/10.1016/j.wear.2023.205111
46. Iyappan SK, Ghosh A. Small Quantity Lubrication Assisted End Milling of Aluminium Using Sunflower Oil. International Journal of Precision Engineering and Manufacturing-Green Technology. 2020;7:337-45. https://doi.org/10.1007/s40684-019-00081-w
47. Hu KH, Hu XG, Wang J, Xu YF, Han CL. Tribological Properties of MoS2 with Different Morphologies in High-Density Polyethylene. Tribology Letters. 2012;47:79-90. https://doi.org/10.1007/s11249-012-9964-1

48. Vazirisereshk MR, Martini A, Strubbe DA, Baykara MZ. Solid Lubrication with MoS2: A Review. Lubricants. 2019;7(57). https://doi.org/10.3390/lubricants7070057